frontiers | Frontiers in Immunology

TYPE Original Research
PUBLISHED 16 October 2023
DOI 10.3389/fimmu.2023.1276255

OPEN ACCESS

EDITED BY
Pedro Augusto Carvalho Costa,
Federal University of Minas Gerais, Brazil

REVIEWED BY
Karen Cerosaletti,
Benaroya Research Institute, United States
Aaron Michels,
University of Colorado, United States

*CORRESPONDENCE
Danijela Tatovic
tatovicd@cardiff.ac.uk

†These authors share senior authorship

RECEIVED 11 August 2023
ACCEPTED 02 October 2023
PUBLISHED 16 October 2023

CITATION
Hanna SJ, Thayer TC, Robinson EJS, Vinh N-N, Williams N, Landry LG, Andrews R, Siah QZ, Leete P, Wyatt R, McAteer MA, Nakayama M, Wong FS, Yang JHM, Tree TIM, Ludvigsson J, Dayan CM and Tatovic D (2023) Single-cell RNAseq identifies clonally expanded antigen-specific T-cells following intradermal injection of gold nanoparticles loaded with diabetes autoantigen in humans.
Front. Immunol. 14:1276255.
doi: 10.3389/fimmu.2023.1276255

Single-cell RNAseq identifies clonally expanded antigen-specific T-cells following intradermal injection of gold nanoparticles loaded with diabetes autoantigen in humans

Stephanie J. Hanna[1], Terri C. Thayer[1,2], Emma J. S. Robinson[1], Ngoc-Nga Vinh[3], Nigel Williams[3], Laurie G. Landry[4], Robert Andrews[1], Qi Zhuang Siah[5], Pia Leete[6], Rebecca Wyatt[6], Martina A. McAteer[7], Maki Nakayama[4], F. Susan Wong[1], Jennie H. M. Yang[8], Timothy I. M. Tree[8], Johnny Ludvigsson[9], Colin M. Dayan[1†] and Danijela Tatovic[1*†]

[1]Division of Infection and Immunity, Cardiff University School of Medicine, Cardiff, United Kingdom, [2]Department of Biological and Chemical Sciences, Roberts Wesleyan University, Rochester, NY, United States, [3]Division of Psychological Medicine and Clinical Neurosciences, Centre for Neuropsychiatric Genetics and Genomics, Cardiff University, Cardiff, United Kingdom, [4]Barbara Davis Center for Childhood Diabetes, University of Colorado, Denver, CO, United States, [5]John Radcliffe Hospital, Oxford University Hospitals NHS Trust, Oxford, United Kingdom, [6]Department of Clinical and Biomedical Sciences, University of Exeter, Exeter, United Kingdom, [7]Department of Oncology, University of Oxford, Oxford, United Kingdom, [8]Department of Immunobiology, School of Immunology & Microbial Sciences, King's College London, Guy's Hospital, London, United Kingdom, [9]Division of Pediatrics, Department of Biomedical and Clinical Sciences, Faculty of Medicine and Health Sciences and Crown Princess Victoria Children´s Hospital, Linköping University, Linköping, Sweden

Gold nanoparticles (GNPs) have been used in the development of novel therapies as a way of delivery of both stimulatory and tolerogenic peptide cargoes. Here we report that intradermal injection of GNPs loaded with the proinsulin peptide C19-A3, in patients with type 1 diabetes, results in recruitment and retention of immune cells in the skin. These include large numbers of clonally expanded T-cells sharing the same paired T-cell receptors (TCRs) with activated phenotypes, half of which, when the TCRs were re-expressed in a cell-based system, were confirmed to be specific for either GNP or proinsulin. All the identified gold-specific clones were $CD8^+$, whilst proinsulin-specific clones were both $CD8^+$ and $CD4^+$. Proinsulin-specific $CD8^+$ clones had a distinctive cytotoxic phenotype with overexpression of granulysin (GNLY) and KIR receptors. Clonally expanded antigen-specific T cells remained *in situ* for months to years, with a spectrum of tissue resident memory and effector memory phenotypes. As the T-cell response is divided between targeting the gold core and the antigenic cargo, this offers a route to improving resident memory T-cells formation in response to vaccines. In addition, our scRNAseq data indicate that focusing on clonally expanded skin infiltrating T-cells recruited to intradermally injected antigen is a highly efficient method to enrich and identify antigen-

specific cells. This approach has the potential to be used to monitor the intradermal delivery of antigens and nanoparticles for immune modulation in humans.

KEYWORDS

nanoparticles, proinsulin peptide, type 1 diabetes, immunomodulation, scRNAseq

1 Introduction

Antigen-specific immunotherapy (ASI) for Type 1 diabetes (T1D) aims to abrogate the immune response to β-cell antigens, without systemic dampening of the immune system. In a Phase 1 safety study to assess the use of ultra-small (< 5nm) gold nanoparticles (GNPs) for this indication, we conjugated the proinsulin peptide C19-A3 to the gold core via a thiol linker and injected these C19-A3 GNPs intradermally using a clinically approved microneedle delivery system, MicronJet600. We have reported elsewhere on the preclinical data associated with this formulation (1) and the clinical results of the trial (2). Proinsulin peptide C19-A3 has been reported to be HLA-DR4 (DRB1*0401) restricted and, given intradermally, with or without GNP, has been shown to be safe (2, 3). When given alone, it demonstrated the potential for tolerance induction in recipients with T1D (4). *In vitro* experiments demonstrated that conjugation of diabetogenic peptides to GNPs facilitated their uptake by antigen presenting cells, particularly Langerhans cells in the skin (1), which have been shown to have tolerogenic properties in some studies (5, 6). In the Phase 1 trial, five participants with newly diagnosed T1D received multiple rounds of C19-A3-GNP and we found persistent reactive immune infiltrate at the C19-A3 GNP injection site (2).

This provided the unique opportunity to analyze the antigen specificity and phenotype of the tissue infiltrate, rather than the historical approach of peripheral blood analysis, where autoantigen-specific cells are very rare, representing ~0.01% of the total T-cell population (7–9). Consequently, the characterization of these cells is challenging and represents a barrier to monitoring antigen-specific T-cell phenotypes during diabetes development, progression, and treatment with novel immunotherapies (10). Much work on antigen-specific cells in T1D has used tetramers to isolate antigen-specific cells from the peripheral blood (8), but is limited by HLA restriction and to known antigen epitopes (11). An alternative approach has been to use *in vitro* stimulation of cells from the peripheral blood with whole diabetes autoantigens or peptides (7, 12, 13) and these studies have suggested that diabetes autoantigen epitopes and HLA restriction exhibit considerable diversity. However, issues of low cell frequency remain with these assays.

In other autoimmune diseases, many insights have come from extraction of lymphocytes from the site of disease, such as from the synovium in psoriatic arthritis. These cells of predominantly memory phenotype are also found in the blood of affected individuals (14). In T1D, whilst antigen-specific lymphocytes are enriched in the pancreas and pancreatic lymph node, these tissues are inaccessible, and thus only suitable for analysis in deceased donors. However, it has been demonstrated that T-cells, particularly $CD8^+$ T-cells, that infiltrate the pancreatic islets in T1D are highly clonal (15–19).

Here we report the characterization of tissue immune cell responses following intradermal injection of C19-A3 GNP, using a state-of-the art method of single cell RNA sequencing (scRNAseq) (16).

2 Materials and methods

2.1 Study design

As described before (2), the Enhanced Epidermal Antigen Specific Immunotherapy Trial -1 (EEASI) study was a two-centre, open-label, uncontrolled, single-group first-in-human Phase 1A safety study of C19-A3 GNP peptide in individuals with T1D (https://clinicaltrials.gov/ct2/show/NCT02837094). The investigational medicinal product (IMP) was C19-A3 GNP (Midacore™), which comprises Midacore™ GNPs (Midatech Pharma Plc, Cardiff, UK) (1, 20) of a size of less than 5 nm, covalently coupled to an 18-amino acid human peptide, the sequence of which is identical to the residues from position 19 in the C-peptide of proinsulin through to position 3 on the A-chain of the same molecule (GSLQPLALEGSLQKRGIV). The peptide is synthesised with a linker to facilitate binding to the GNPs: 3-mercaptopropionyl-SLQPLALEGSLQKRGIV 2 acetate salt (disulfide bond). The chemical composition of the IMP contained a ratio of 4 C19-A3 peptides: 11 glucose C2: 29 glutathione ligands as determined by 1H-NMR (proton nuclear magnetic resonance). A typical batch contained: [C19-A3 peptide] = 1.33 mg/ml; [gold] = 5.5 mg/ml; [glucose linker] = 0.6 mg/ml; [glutathione linker] = 1.79 mg/ml. As the drug substance was diluted 1:7 to 1:10, depending on the content of C19-A3 peptide per particle, and as 50 µl of the diluted solution was administered to the study participants, this corresponded to C19-A3 peptide: 10 µg; gold: 39 µg; glucose linker: 4.3 µg; glutathione: 12.7 µg.

Participants diagnosed with T1D and confirmed to possess the *HLA-DRB1∗0401* genotype, were given three doses of C19-A3 GNP

at 4-weekly intervals (weeks 0, 4, and 8) in the deltoid region of alternate arms (2 doses in one arm and 1 dose in the other arm) via CE-marked 600 µm length MicronJet600™ hollow microneedles (NanoPass Technologies Ltd. Israel) attached to a standard Luer-lock syringe. The single-dose given in 50 µl volume was equivalent to 10 µg of C19-A3 peptide.

The planned duration of the study was initially 20 weeks, but this was later extended to 52 weeks to continue safety follow-up of the participants due to a persistent local response to the intradermal injection (as described below). Skin changes at the injection site were followed up beyond 52 weeks in some individuals (12-28 months) and additional analyses were performed to determine the nature of these changes, which are the focus of this manuscript. Data on safety and metabolic effects following C19-A3 GNP administration has been published separately (2). Study participants are denoted by the prefix EEASI, followed by their study number in the results section.

2.2 Blood samples

PBMCs were isolated on Ficoll–Paque Plus (1.077 6 0.001 g/ml, +20°C; GE Healthcare Biosciences, Sweden) gradient centrifugation from the peripheral blood of participants. Samples were cryopreserved in CryoStor® (Sigma-Aldrich, Gillingham, UK) on the day of the collection and thawed on the day of the experiment.

2.3 Suction blisters

Skin suction blisters were raised as described previously (21). Briefly, suction cups were applied to the deltoid region of participants' arms, at the site of previous injection. Skin suction blisters were performed by gradually applying negative pressure (up to 60 kPa) from a suction pump machine VP25 (Eschmann, Lancing, UK) through a suction blister cup with a 15-mm hole in the base (UHBristol NHS Foundation Trust Medical Engineering Department, Bristol, UK) for 2–4 hr until a unilocular blister had formed within the cup. The cup was left in place for a further 30-60 minutes to encourage migration of lymphocytes into the blister fluid. The cup was then removed, and the blister fluid aspirated using a needle and syringe. Blister fluid was immediately suspended in 10ml heparinized RPMI (Gibco)+ 5% fetal calf serum Cells were counted then washed once and resuspended in an appropriate volume for scRNAseq. Samples were used fresh on the day of the collection.

2.4 Punch biopsies

Punch skin biopsies of the local area were performed under aseptic conditions and under local anesthetic (Lidocaine Hydrochloride Injection BP 2%, w/v), using a 6-mm sterile disposable biopsy punch. Following the biopsy, samples were divided with half immediately placed in 10% formalin and transported to the laboratory and the other half placed in RNA later™ (Fisher Scientific, Loughborough, UK) for bulk RNA sequencing.

Control skin samples were obtained from female patients aged 19–82 years, following mastectomy or breast reduction after informed consent. Skin without obvious pathological findings, which was surplus to diagnostic histopathology requirements, was used in the experiments. Control punch biopsy samples were treated in the same manner as described above.

2.5 Immunofluorescence confocal microscopy

4mm sections of formalin-fixed paraffin-embedded skin biopsies were examined via immunofluorescence protocols. In brief, sections were dewaxed with Histoclear™ (Fisher Scientific, UK), rehydrated in an ethanol series (100%,90%,70%,50% and ddH_2O) and underwent dual antigen retrieval protocols (namely, heated under pressure for 20mins in 10mM Citrate (pH6 buffer) and 20mins in 1mM EDTA (pH8)). Sections were then blocked with 5% normal goat-serum (Vector, UK), and serially stained with multiple combinations of antibodies specific for CD8, CD20 and Ki67 (Dako: 1:50 (#M7103); 1:700 (#M0755); and 1:400 (#M7240), respectively), and FoxP3, CD4, CD103 and CD11c (Abcam: 1:80 (#ab133616); 1:100 (#ab20034), 1:100 (#129202), 1:200 (#ab52632), respectively) – each being incubated at 4°C overnight. Antigen binding by primary antibodies was detected via HRP-conjugated species-specific secondary antibodies (rabbit or mouse), which were then visualized with tyramine-bound Alexa-488, 555 and 647 fluorescent dyes (Thermofisher tyramide Superboost kits: B40912, B40922, B40913, B40923, B40916, B40926)). Each antigen was examined in at least 2 complementary combinations to ensure comprehensive understanding of expression and for quality control (eg CD8 was examined in the following combinations: CD8/CD103/Ki67; CD8/CD103/FoxP3; CD8/CD103/CD11c; CD8/CD4/FoxP3 and Ki67 was examined CD20/CD4/Ki67 and CD8/CD103/Ki67. Imaging was carried out using an SP8 DMi8 Confocal Laser scanning microscope, where 6 fields of view were imaged for each combination in every section to capture an accurate overview of the whole biopsy. Images were analyzed and mean numbers of relevant immunostained cells were captured using Halo™ Highplex module (Indica Labs, USA). Cell counts verified by manual counts in 25% of the images by two independent researchers in a blinded manner.

2.6 RNA sequencing of punch biopsies

After cutting skin samples into small pieces, samples were homogenized and lysed by using Tissue Raptor II and QIAzol® Lysis protocol (QIAzol® Handbook 2021, QIAgen, Crawley, UK). The quality of RNA was routinely assessed by determining the A260:A280 ratio using NanoDrop2000 (Thermo Scientific, UK). RNA libraries were created using TruSeq stranded Total RNA with ribozero GOLD (illumina, UK) and sequenced on an illumina HiSeq 2500 platform with 2 x 75 bp reads to the depth of 13.5-22.8 million reads per sample.

2.7 scRNAseq

Samples were processed using a 10xGenomics V1 human 5'GEX kit and libraries were constructed following standard 10xGenomics protocols. Samples were pooled and sequenced on Illumina NextSeq and MiSeq. scRNAseq libraries were sequenced aiming for 20,000 reads per cell for GEX and 5,000 reads/cell for VDJ.

Demultiplexed samples were processed individually using the 10xGenomics CellRanger 3.0.2 pipeline and GRCh38-1.2.0. Data were further processed using the Seurat V3 package in R (22). QC was performed according to standard Seurat pipeline, with cells with less than 500 nFeatures (unique genes expressed) removed. This resulted in the removal of contaminating RBCs. DoubletFinder (23) was used to remove doublets. After QC, for EEASI-A, B and C respectively, mean nFeatures were 1491, 1090, 1195 and mean nCountRNA (number of UMIs detected) were 4570, 3092, 2965, mean percentage mitochondrial genes were 4.25, 4.56, 3.18.

TCR clonotypes were assigned using the CellRanger pipeline such that a shared clonotype required identical V and J gene usage, and identical CDR3 sequence at the nucleotide level. However, nucleotide differences in the V or J gene outside the CDR3 region were allowable within a clonotype. TCR sequences and clone numbers were added to the Seurat object metadata slot. TCR clone numbers refer to data generated in the CellRanger pipeline, even if clones of the same cell did not meet gene expression quality control thresholds. Raw data contained red blood cells, but these were removed automatically in the quality control (QC) process due to low levels of unique molecular identifiers (UMIs) and low unique genes identified. Cell clusters were determined by Seurat, and the $CD4^+$ T-cell cluster was manually divided in to Tregs and memory $CD4^+$ T-cells. TCRs were screened against VDJDB (24) and McPas (25) databases using the immunarch package in R.

2.8 Antigen specificity experiments

TCR specificity was determined as previously described (26, 27). Briefly, TCR consensus sequences were obtained from the CellRanger output (consensus sequences being the most widely expressed clonotype including point mutations sequenced in the V and J genes but outside the common CDR3 region). TCR α-chain and β-chain genes, connected by the porcine teschovirus-1 2A peptide gene, were engineered into a murine stem cell virus–based retroviral vector. T-cell transductants were generated by retroviral transduction of the 5KC murine T-cell hybridoma cells lacking endogenous TCR expression and expressing human CD4 or CD8 according to the original T-cell phenotype. The 5KC cells also incorporate an NFAT-binding sequence followed by the fluorescent ZsGreen-1 gene, such that activation of the cells can be detected by flow cytometry (28). 5KC cells were spin-infected with replication-incompetent retroviruses that were produced from Phoenix cells transfected with the retroviral vectors and the pCL-Eco packaging vector. Only cells that successfully expressed TCRs express CD3 on the cell surface. Cells transduced with retroviruses were therefore selected by sorting for CD3 expression (CD3ϵ MicroBead Kit, mouse, Miltenyi Biotec) to select transduced cells. Successful transduction was further confirmed by positive response to αCD3αCD28 dynabeads.

5KC cells bearing TCRs were incubated with autologous EBV-transformed B cells with antigens or blocking antibodies as indicated at $1x10^6$ 5KC/ml and $1x10^6$ EBV-transformed B cells/ml in 200µL RPMI 1640 (Gibco)+penicillin/streptomycin (Gibco) +10% foetal calf serum (BioSera)+ 2-Mercaptoethanol (Thermo Fisher Scientific) in 96-well round bottomed plates. The positive control was 5µL αCD3/CD28 microbeads (Dynabead). The proinsulin (PI) used in these studies was a recombinant human PI and was a kind gift from Luciano Vilela, Biomm S.A., Brazil. The recombinant human PI has the same structure and amino acid sequence as that of the native human PI, but also incorporates a histidine affinity tag (sequence from N′ to C′: MAHHHHHHMGR), resulting in a total of 97 amino acids and a molecular weight of approximately 12,500 g/mol (personal communication Luciano Vilela) (29). C19-A3 GNP (Midacore™) has been previously described (2). Gold nanoparticles 5nm diameter were from Merck Life Sciences. Ultra-LEAF Purified anti-human HLA-DR Antibody [Clone: L243] and Ultra-LEAF Purified anti-human HLA-A,B,C Antibody [Clone: W6/32] were from Biolegend and used at a 1:800 dilution in cell culture. Flow cytometry was performed to evaluate the expression of NFAT-reporter fluorescent protein on a BD Canto II after 24h. Murine IL-2 ELISAs were performed on undiluted cell culture media following the manufacturer's instructions (Biolegend) after 48h. Results were analyzed using R.

2.9 Statistics

Plots and Statistics were carried out in GraphPad Prism version 9.5.0 for analysis of confocal microscopy images.

Unpaired T tests with FDR correction were used to compare gene expression of specific markers in punch biopsies between healthy controls and clinical trial participants. DEG pathway analysis was conducted using Metascape standard parameters (28) on all DEG with an FDR less than 0.05.

DEGs that defined cell clusters in Seurat were determined using Seurat's inbuilt statistical methods using the Wilcoxon rank sum test. DEG pathway analysis was conducted using Metascape standard parameters (28) on all DEG with an uncorrected p value less than 0.05.

2.10 Ethics statement

This study was carried out with the approval of the UK Research Ethics Service, the Linköping Regional Research Ethical Review Board (RERB), the UK Medicines and Healthcare products Regulatory Agency (MHRA) for Clinical Trial Authorisation, and the Swedish Medical Products Agency (MPA). Written informed consent was obtained from all participants. The trial was conducted in compliance with the principles of the Declaration of Helsinki (1996) and the principles of Good Clinical Practice and in

accordance with all applicable regulatory requirements including but not limited to the Research Governance Framework and the Medicines for Human Use (Clinical Trial) Regulations 2004, as amended in 2006. Further details are available at https://clinicaltrials.gov/.

3 Results

3.1 Study participants

A total of five participants who received intradermal microneedle injection of C19-A3 GNP were included in the final analysis. Whilst four participants received 3 doses of C19-A3 GNP, one participant (EEASI-C) received only the first dose due to the decision to halt further drug administration. As previously described, all participants were autoantibody-positive defined by being positive to at least one of GADA, IA-2A, or ZnT8A and possessed HLA-DRB1∗0401 genotype (2). Two participants had a punch biopsy of the injection sites, 3 months after injection in one (participant EEASI-B) and 7 months after injection in another participant (participant EEASI-A). Three participants had a suction blister raised over the injection sites: 10 months after injection in two participants (participants EEASI-B and EEASI-C) and 28 months after injection in the third participant (participant EEASI-A) – Supplementary Table 1.

3.2 Intradermal injection of C19-A3 GNP results in sustained GNP deposits in the skin and immune cell infiltration

As previously reported (2), C19-A3 GNP injections induced formation of a dark-coloured bleb (diameter 3–4 mm) (Figure 1A) in all participants, with transient surrounding erythema lasting up to 60 min post injection. The dark area persisted and reduced in size to 1–2 mm by the following day. Subsequently, delayed skin changes over the injection site were observed. The change consisted of a small central area of GNP-derived pigmentation surrounded by persistent asymptomatic circular erythematous induration. Induration initially reached 2–3 cm in diameter, which then reduced to approximately 1 cm during the follow-up period. These delayed reactions appeared 17.4 ± 2.3 days after the first injection, but much sooner, i.e. 1–3 days after the second and third injection, a reaction that was consistent in all participants. The skin changes faded significantly over the course of the study, although they were still visible at the end of the observation period (12–24 months depending on the participant).

A skin biopsy of the injection site was performed on two participants (3 months after injection in one (participant EEASI-B) and 7 months after injection in another participant (participant EEASI-A)). Confocal microscopy showed that $CD8^+$ T-cells predominated in all parts of the immune clusters (Figures 1B, C) with total overall counts as follows $CD8^+$=6537, $CD4^+$=1526, $CD20^+$=1363/1.54mm^2 area. $CD8^+$ T-cells proportionally contained higher numbers of $Ki67^+$ cells in comparison to $CD20^+$ and $CD4^+$ cells (Figure 1D). There was also evidence of intradermal gold retention as previously reported (2).

To examine the characteristics of the cells that were involved in the injection site reaction, we formed suction blisters at the injection site in three participants and performed scRNAseq and TCR VDJ sequencing on the cells in the blister fluid. After quality control and doublet removal, cells were visualized using a UMAP projection (Figure 2A). Cell types identified included memory $CD8^+$ T-cells, memory $CD4^+$ T-cells, Tregs, dendritic cells, melanocytes and keratinocytes. The findings were consistent across all three participants (Figure 2B).

The cell types labelled in the UMAP projections were those that were clustered automatically using Seurat, with the exception of the $CD4^+$ memory T-cells and Treg cells, which were initially a single cluster. This cluster was manually gated into two groups and the top 10 DEGs were used to discern the separate phenotypes. This revealed a distinct $FOXP3^+$, $CTLA4^+$, $TIGIT^+$ population of Tregs, whereas the other $CD4^+$ cells had a memory phenotype (Supplementary Figure 1A). The remaining $CD8^+$ T-cells clustered into five groups and were defined using known phenotypic markers: 1. T_{EM} – T-cell effector memory comprised the largest subset that expressed CD69, granzyme B (GzB), perforin. They also expressed PD-1; 2. $T_{RM/EM}$ – a subset of true tissue resident T-cells with some characteristics of effector memory, which express CD103 and CD69. They are proliferating ($KI67^+$) and are $CXCR3^+$, and GZB^+; 3. T_{RM}- T-cell resident memory that expressed CD69, CD27 and PD1, but did not demonstrate cytotoxic gene expression; 4. T_{PM} - peripheral memory T-cells that express CD69 but also CD62L, CCR7 and CD127 having characteristics of both naïve and memory cells. They lack cytotoxic or cytokine gene expression; 5. γδ and Granulysin $(GNLY)^+$ $CD8^-$ highly cytotoxic effector memory $CD69^+$, expressing GNLY, GzB, perforin. They are $CD127^+$, and express XCL1 and CXCR3. (Supplementary Figure 1). B-cells were not detected in the blister fluid, despite being abundant in the punch biopsies and this was likely to be due to a reduced ability to migrate into the fluid in the timescale of the blister formation.

3.3 Single cell RNAseq analysis of T-cells harvested from the injection site reveals significant clonal expansions specific for the injected antigens

We examined the sequences of the paired α-and β-chains of the TCRs for each T-cell (TCR clonotype). In addition, there were cells that shared the TCRβ with other clones but lacked a sequenced α-chain as the mRNA for the α-chain is less abundant in T-cells (30). TCR clonotypes were assigned using the CellRanger pipeline such that a shared clonotype required identical V and J gene usage, and identical CDR3 sequence at the nucleotide level. However, nucleotide differences in the V or J gene outside the CDR3 region were allowable within a clonotype. Where only one chain was present this was assigned as a separate clonotype to those with an identical chain but an additional chain also detected. A striking feature was the presence of a large number of clonally expanded T-

10.3389/fimmu.2023.1276255

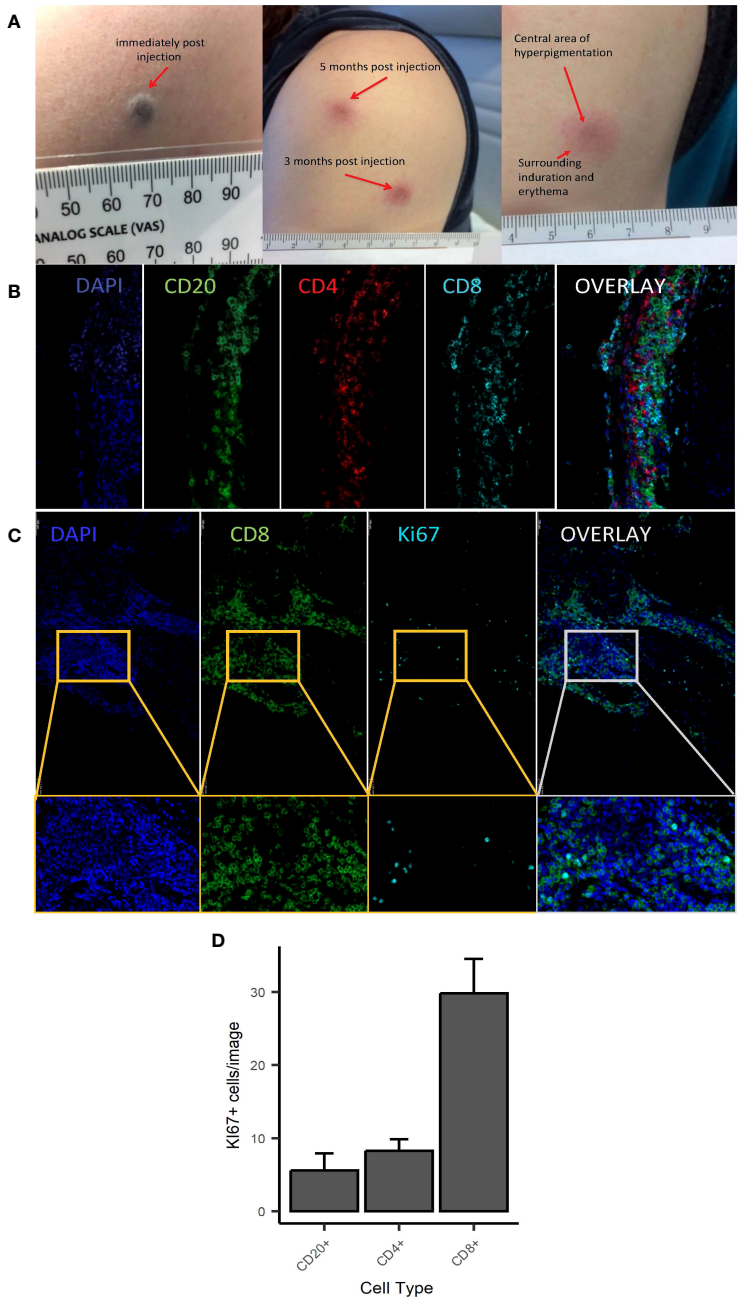

FIGURE 1
Macroscopic and microscopic appearance of skin changes following intradermal injection of C19-A3 GNP. **(A)** Images show representative injection sites in deltoid region immediately after injection (left), several months after injection (centre) with the enlarged image showing dark centre and surrounding erythematous induration (right); **(B, C)** Sections from punch skin biopsies of participants EEASI-A and EEASI-B were stained for CD20, CD4, CD8 and Ki-67 and imaged with a fluorescence confocal microscope. Six fields of view were analysed. $CD8^+$ T Lymphocytes predominated in all parts of the immune clusters: total overall counts/1.54mm^2 area: $CD8^+$=6537, CD4+=1526, $CD20^+$=1363/1.54mm^2; **(D)** number of $Ki67^+$ cells (expressed as mean+/-SEM) was higher amongst $CD8^+$ cells (29.83+/-4.65) vs $CD20^+$ (5.58+/-2.33) and $CD4^+$ (29.83+/-4.65) cells. Punch biopsies were performed 7 and 3 months after injection in participants EEASI-A and EEASI-B, respectively.

cells sharing the same paired TCRs. These clonal expansions were frequently very large. In the case of EEASI-C the largest expansion comprised 52 clonally identical cells, out of a total of 807 cells with sequenced TCRs (Figure 2D and Table 1). The phenotypes of the clonally expanded T-cells included memory $CD4^+$ T-cells, Tregs, $CD8^+T_{TR/EM}$, $CD8^+T_{EM}$, $CD8^+T_{PM}$, and $CD8^+T_{RM}$ (Figures 2C, D) but not γδ and GNLY+ $CD8^+$ T-cells. Two of the three participants had clones falling into all compartments listed above. However, EEASI-B had only $CD8^+T_{EM}$ expanded clones (Figure 2D).

Next, we wished to determine whether the clonally expanded T-cells had TCRs specific for the injected antigen. Hence, from each participant we selected clonally expanded TCRs to re-express in an *in vitro* cell based system (27, 31). We based the decision on which sequences to select on the size of the clonal expansions (with $CD8^+$

10.3389/fimmu.2023.1276255

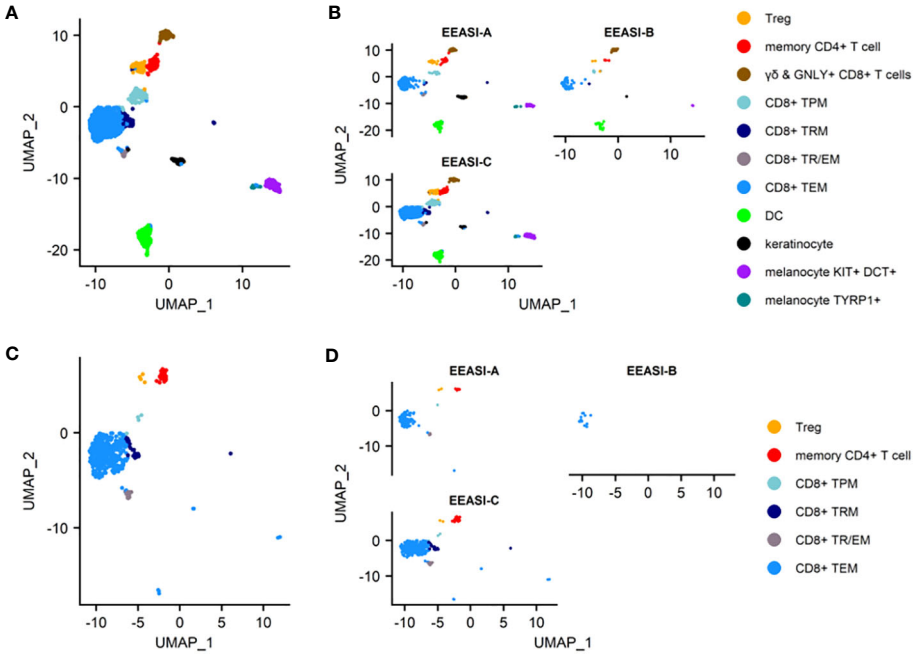

FIGURE 2
scRNAseq reveals memory T-cell infiltration of injection site of C19-A3 GNP and clonal expansions **(A)** UMAP plot of pooled samples of cells from the blister fluid of 3 donors **(B)** UMAP plots of the blister fluid cells split by donor; **(C)** UMAP plot of all clonally expanded T-cells in the blisters (clones share an identical TCRα and TCRβ CDR3 at nucleotide level, and V and J gene usage, or where one chain is not detected, the remaining chain is identical); (D) UMAP plot of clonally expanded T-cells in the blister split by donor. Suction blisters were performed in three participants EEASI-A, EEASI-B and EEASI-C, 28, 10 and 10 months after injection, respectively. T_{EM} -effector memory T-cell, T_{RM} – tissue resident T cells, $T_{TR/EM}$ – true tissue resident T-cell with some characteristic of effector memory, T_{PM} – peripheral memory T-cell, Treg – T regulatory T-cell, DC – dendritic cell.

T-cells having the largest expansions) as well as including smaller expansions of memory $CD4^+$ (maximum expansion of 6 cells) and Treg cells (maximum expansion of 3 cells).

We re-expressed the TCRs in a mouse T-cell hybridoma, 5KC (31), expressing and challenged them with C19-A3 GNP, gold nanoparticles (GNP) and whole proinsulin (PI). Of 22 TCRs remade we found five that were GNP-reactive, and six that were proinsulin-reactive. A T-cell clone with two β-chains and a single α-chain was specific only with one of the β-chains (EEASI-B:Bl-4-proinsulin specific; EEASI-B:Bl-5 unknown specificity) (Figure 3A, B and Table 1). Recognition of proinsulin and GNP were HLA-restricted as illustrated by clones EEASI-A:Bl3 (GNP- reactive HLA-A01:01 restricted) and EEASI-C:Bl6 (PI reactive, HLA-DR restricted) (Supplementary Figure 2). Reactivity of re-expressed TCRs to whole proinsulin rather than C19-A3 peptide, as responses to C19-A3 were generally weaker (data not shown). No clonotypes were exactly shared between donors. We then screened the TCRs against VDJDB (24) and McPas (25) databases. Of the re-expressed TCRs five had single TCR chains in the databases. Of these two were GNP specific alpha chains, one reported to recognize EBV, and one reported to recognize both MLANA and CMV. One was a proinsulin specific beta chain, found in CD4+ T cells in our study but reported to recognize influenza in a HLA-A*0201 restricted fashion (found in both McPAS and VDJDB) and CMV with a HLA-C*07:02 restriction. Two TCRs we found to be non-specific had alpha chains reported to recognize CMV. (Supplementary Table 2). Examining all sequenced TCRs, clonally expanded TCRs were not disproportionately found in the databases. Nor was there a convincing trend for expanded TCRs to be more cross re-active than non-expanded TCRs. For example whilst EEASI-A clonotype 10 alpha chain CAVTDSNYQLIW had a clonal expansion of three and was found in the databases to bind tuberculosis, human BST2 and CMV, EEASI-A clonotype 55 alpha chain CAVRDSNYQLIW with a clonal expansion of one, was found in the databases to bind peptides from CMV and three from EBV as well as HIV, BST2 and Streptomyces KanJ (Supplementary Table 3).

3.4 Phenotype of clonally expanded T-cells differs depending on antigen-specificity

All the identified GNP-specific clones were $CD8^+$, whilst PI specific clones were both $CD8^+$ and $CD4^+$. The majority of clones of unknown specificity were $CD8^+$ with one exhibiting $CD4^+$ Treg phenotype (Table 1, Figure 4). Additionally, many clonotypes had more than one phenotype. For example, some clones were found in both $CD8^+T_{EM}$ and $CD8^+T_{RM/EM}$ clusters, suggesting some plasticity of phenotype.

We next compared differentially expressed genes (DEG) between clones of unknown antigen specificity, GNP-reactive clones and proinsulin reactive clones (Supplementary Figure 3). As the majority of re-expressed TCRs from $CD4^+$ T-cells were PI specific, it was not possible to compare differentially expressed genes between PI-specific and other specificity $CD4^+$ T-cells. For

TABLE 1 Phenotype, reactivity, TCR sequences and number of copies of the clones harvested from the blister fluid raised over the C19-A3 GNP injection sites.

Donor	TCR ID	Clonal expansion	T cell origin	Specificity	TCRα	TCRβ	TRAV	TRAJ	TRBV	TRBD	TRBJ	TRBC
EEASI-A	EEASI-A:Bl1	23	CD8	non	CAVRGFGNEKLTF	CASSETPAPNYGYTF	21	48	9	–	1-2	C1
EEASI-A	EEASI-A:Bl2	11	CD8	GNP	CAPRESSYKLIF	CASSLGRAAGGETQYF	21	12	5-6	D2	2-5	C2
EEASI-A	EEASI-A:Bl3	7	CD8	GNP	CAVKNYGQNFVF	CSVVTHYGYTF	12-2	26	29-1	–	1-2	C1
EEASI-A	EEASI-A:Bl4	7	CD8	GNP	CAENADMRF	CASSLDRGGSPLHF	13-2	43	11-2	D2	1-6	C1
EEASI-A	EEASI-A:Bl5	6	CD8	GNP	CAVDTGRRALTF	CAIPLAMNTEAFF	21	5	2	D2	1-1	C1
EEASI-A	EEASI-A:Bl7	4	CD8	non	CATDTNTGNQFYF	CASNRGWSPGTYEQYF	17	49	27	D2	2-7	C1
EEASI-A	EEASI-A:Bl8	2	CD4Treg	non	CAVRDYSNSGYALNF	CSARVQGTPNIQYF	1-2	41	20-1	D2	2-4	C1
EEASI-A	EEASI-A:E4	2	CD4	PI	CALNTPYSGAGSYQLTF	CASSLTSGNEQFF	9-2	28	7-9	D2	2-1	C2
EEASI-B	EEASI-B:Bl-1	2	CD8	non	CAVRGSGGYQKVTF	CSAISYNEQFF	12-2	13	20-1	–	2-1	C2
EEASI-B	EEASI-B:Bl-2	2	CD8	non	CLVVRDSWGKLQF	CASSPNRGTSGGGTYNEQFF	4	24	11-2	D2	2-1	C2
EEASI-B	EEASI-B:Bl-3	1	CD8	GNP	CAVNAGTGANNLFF	CASSLGGPEQYF	8-1	36	7-2	D2	2-7	C2
EEASI-B	EEASI-B:Bl-4*	1	CD8	PI	CAVNEGTGANNLFF	CATIRFQGPWGEQFF	8-1	36	24-1	D1	2-1	C2
EEASI-B	EEASI-B:Bl-5*	1	CD8	non	CAVNEGTGANNLFF	CASSLGGPEQYF	8-1	36	7-2	–	2-3	C2
EEASI-C	EEASI-C:Bl-1	52	CD8	non	CAGRSNDYKLSF	CASALSGSYNEQFF	25	20	7-2	–	2-1	C2
EEASI-C	EEASI-C:Bl-2	13	CD8	non	CAVNAGSGAGSYQLTF	CAIREGQGARNEQFF	8-1	28	10-3	D1	2-1	C2
EEASI-C	EEASI-C:Bl-3	11	CD8	non	CATPLGGANSKLTF	CAISEGAEQFF	17	56	10-3	D1	2-1	C2
EEASI-C	EEASI-C:Bl-4	11	CD8	PI	CALIDTGRRALTF	CATSASSGSNQPQHF	6	5	24-1	D1	1-5	C1
EEASI-C	EEASI-C:Bl-5	7	CD8	non	CEGGSYIPTF	CASSQETSGVGGNIQYF	17	6	4-3	D2	2-4	C2
EEASI-C	EEASI-C:Bl-6	6	CD4	PI	CATDESNYQLIW	CASSPGLAYETQYF	17	33	7-2	D2	2-5	C2
EEASI-C	EEASI-C:Bl-7	6	CD8	non	CAVAMNSGYSTLTF	CASSEGGTYEQYF	20	11	10-2	D1	2-7	C2
EEASI-C	EEASI-C:Bl-8	3	CD4Treg	PI	CALRSSGNTGKLIF	CASTPTGLAYEQYF	9-2	37	28	D2	2-7	C2
EEASI-C	EEASI-C:Bl-10	6	CD8	non	CAVKSAGNKLTF	CASSVGAAGELFF	8-6	17	9	–	2-2	C2
EEASI-C	EEASI-C:Bl-11	5	CD4	PI	CAMSDWTNAGKSTF	CATSDSLTGVYGYTF	12-3	27	24-1	D1	1-2	C1

*In general, sequenced T-cells had a single TCRα and TCRβ, however, EEASI-B:Bl-4 and EEASI-B:Bl-5 come from a cell with two TCRβ-chains and a single TCRα-chain remade as two separate 5KC cell lines. Non denotes non-specific for either PI or GNP.

10.3389/fimmu.2023.1276255

10.3389/fimmu.2023.1276255

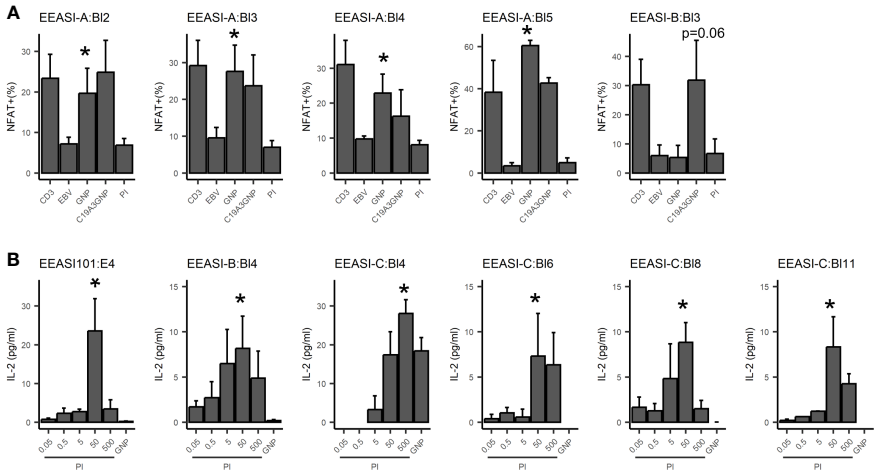

FIGURE 3
Antigen specificity of re-expressed TCRs. TCRs were re-expressed in 5KC cell lines. Each graph represents an individual 5KC cell line with a single TCR. **(A)** GNP reactivity was measured by fluorescent reporter downstream of the NFAT promoter. CD3 - αCD3/CD28 positive control; EBV - patient-autologous EBV transformed cells used to present antigen-negative control; GNP: EBV transformed cells used to present GNP; C19-A3 GNP: EBV transformed cells used to present C19-A3 GNP; EBV transformed cells used to present PI - 50μg proinsulin. Data are pooled from three independent experiments. **(B)** Proinsulin reactivity was assessed by mIL-2 production measured by ELISA, with background mIL-2 from 5KC+ EBV cells alone subtracted. GNP: 25μL GNP, PI: proinsulin concentration in μg/ml. Data are pooled from at least three independent experiments. Values indicate results of unpaired T-tests, *p<0.05.

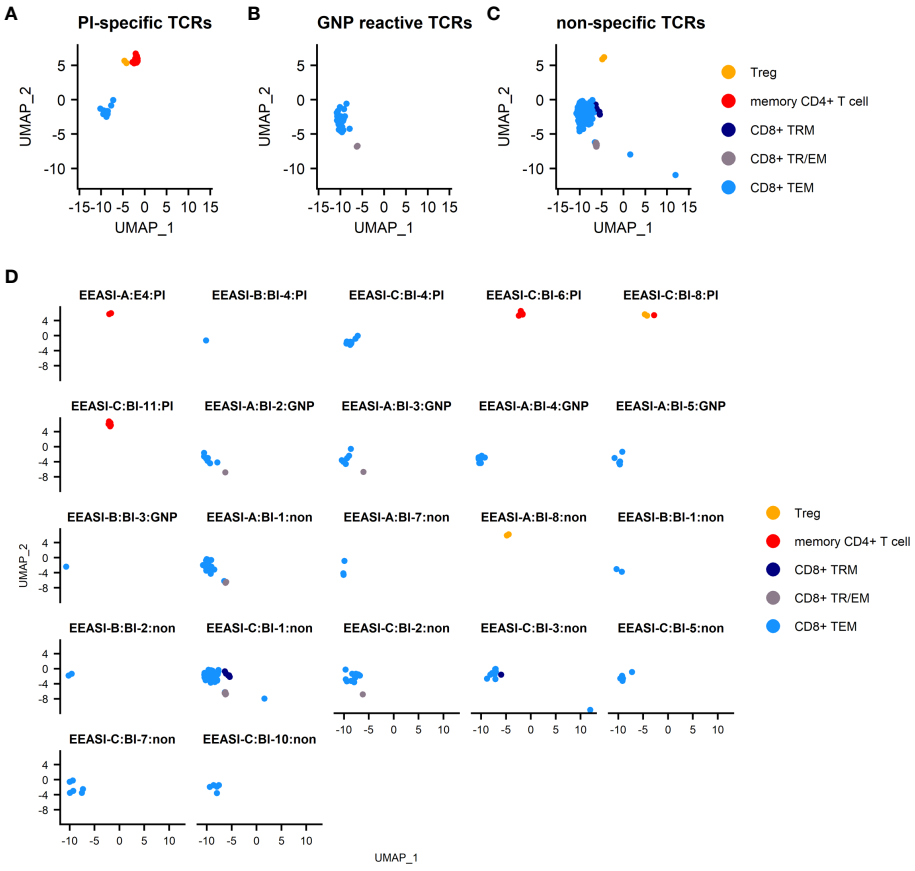

FIGURE 4
Specificities and T-cell phenotypes of clonally expanded cells in blister fluid. **(A)** combined UMAP plot of PI-specific clones; **(B)** combined UMAP plot of GNP-reactive clones; **(C)** combined UMAP plot of clones of unknown specificity; **(D)** UMAP plots of individual T-cell clones. T_{EM} -effector memory T-cell, T_{RM} – tissue resident T cells, $T_{TR/EM}$ – true tissue resident T-cell with some characteristic of effector memory, Treg – T regulatory T-cell.

$CD8^+$ T-cells, Metascape pathway analysis between PI-specific and either gold-specific or non-specific T-cells revealed DEG in pathways associated with adaptive immune system activation and TCR signaling (Supplementary Figure 3). Examination of the top DEG revealed overexpression in PI-specific $CD8^+$ T-cells of GNLY and KIR receptors. (Figure 5).

Despite the high level of specificity for the injected antigens, a limitation of the blister approach was a lack of healthy control individuals. Therefore, in order to determine whether the T-cells present in the blister had been recruited to the skin following injection of antigen, we next compared bulk RNA sequencing of punch biopsies from injection sites to those from healthy control individuals. We first searched canonical markers of leukocytes, T-cell subsets and chemokines and cytokines (Supplementary Figure 4). $CD4^+$ and $CD8^+$ transcripts were significantly upregulated in EEASI participants compared to control participants. The B cell marker CD19 was also upregulated, confirming the presence of B-cells in the confocal microscopy sections. Th1/$CD8^-$ associated genes were particularly upregulated as were Th1-asscoiated chemokines and cytokines. Overall, DEG between T-cells from EEASI and control participants mapped to pathways primarily associated with immune cell activation (Supplementary Figure 4D). To directly correlate between the bulk RNAseq and scRNAseq we obtained a list of the top 10 genes that defined major cell types in the scRNAseq. We then searched for these genes within the punch biopsy RNAseq data and compared between control and EEASI samples. Nine out of 10 T-cell marker genes from the scRNAseq dataset were upregulated in EEASI compared to controls (Supplementary Figure 5A), as were all 10 markers for the $CD8^+T_{EM}$ subset (Supplementary Figure 5B).

4 Discussion

We have demonstrated that intradermal injection of GNP with proinsulin peptide antigenic cargo substantially enriched antigen-specific clonally expanded T-cells in the skin, compared to the frequencies found in the peripheral blood. Using scRNAseq of T-cells harvested from the fluid of blisters raised over the injection sites, we showed that the local T-cell response was directed to the gold core as well as the antigenic cargo. The antigen-specific cells were predominantly $CD8^+$ T-cells with some $CD4^+$ T-cells and had diverse phenotypes, which more resembled cytotoxic tissue resident T-cells than blood T-cells.

We demonstrated reactivity of re-expressed TCRs to whole proinsulin rather than C19-A3 peptide, as responses to C19-A3

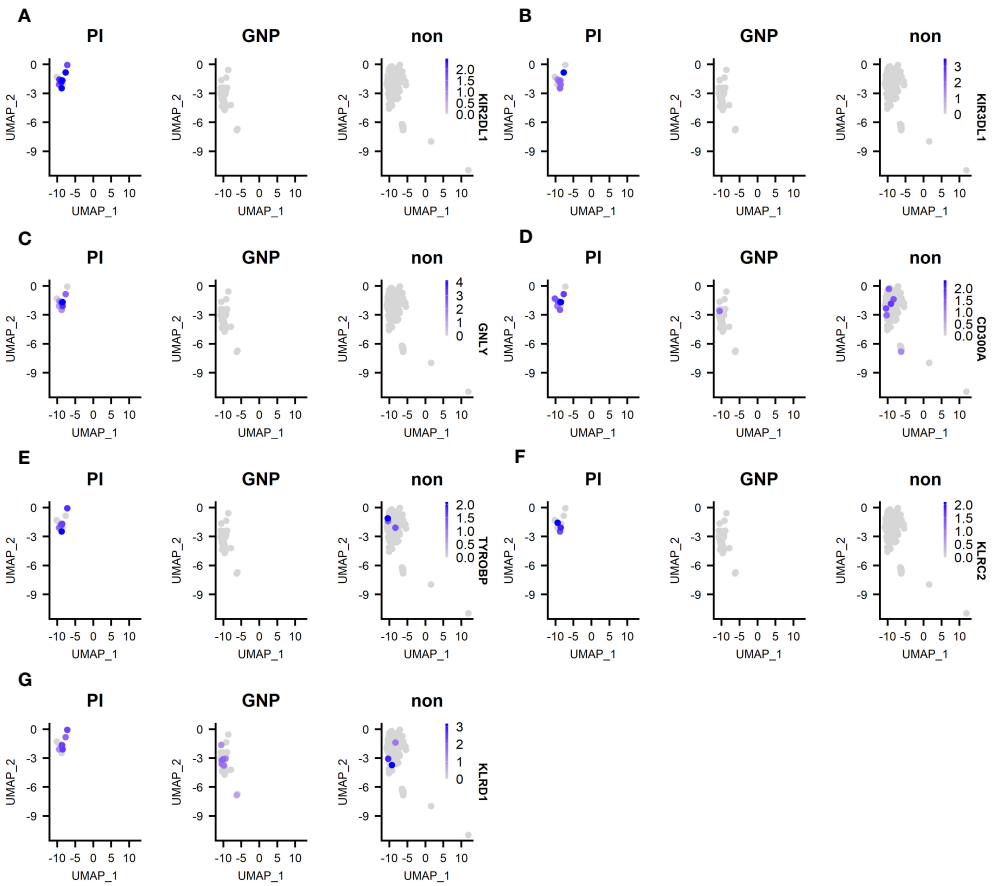

FIGURE 5
Top 5 DEG between PI-specific clones, gold-specific clones and clones of unknown specificity (designated non). **(A)** expression of KIR2 DL1; **(B)** expression of KIR3 DL1; **(C)** expression of granulysin (GNLY); expression of KIR3 DL1; **(D)** expression of CD300A; **(E)** expression of TYROBP; **(F)** KLRC2; **(G)** KLRD1.

were generally weaker (data not shown). This is likely due to the efficacy of autologous EBV-transformed B cells to take up and process whole proteins vs peptide. However, we cannot exclude the possibility that the binding of the C19-A3 peptide to the gold directs its cleavage and presentation within the antigen presenting cells *in vivo*, favoring generation of immunogenic peptide fragments different from those produced *in vitro* from unconjugated C19-A3.

The finding of PI-specific CD8 clones is intriguing given that C19-A3 is known to be an HLA class II-restricted peptide (4, 32). Again, antigen processing to release smaller peptides suitable for HLA class I presentation is a possible explanation. There are limited reports in the literature of $CD8^+$ T-cell epitopes within proinsulin C19-A3. Proinsulin C29-A4 is a reported CD8 epitope for HLA-A*02:01 (33) (expressed by participant EEASI-C in our study (2)). HLA-B15 (expressed by both participants EEASI-B and EEASI-C) is reported to bind Proinsulin C29-A4, C30-A4 and C31-A4 (34) (although tetramer assays for antigen-specific TCRs have not been reported), whilst proinsulin C23-32 is a HLA-A*03 epitope (35) (expressed by donor EEASI-B). A search of IEDB found no known epitopes within C19-A3 that would utilize donor EEASI-A HLA class I types, although many additional CD8 epitopes are known to reside within preproinsulin and to be directly involved in triggering the killing of β-cells (26, 36). Future work will examine the HLA-restriction and peptide epitopes involved for both CD4+ and CD8+ T cells.

In addition to proinsulin specific clones, we identified GNP-specific $CD8^+$ T-cell clones in the blister fluid and were able to demonstrate HLA-restricted reactivity. However, none of the re-expressed $CD4^+$ TCRs were GNP-specific. As an element, gold is inert and unreactive, and requires ionization to function as a hapten (37). This may have occurred due to the addition of linkers (glutathione and glucose) to the GNPs used in this study and the subsequent cleavage of the linkers either intracellularly or extracellularly.

Gold-reactive TCRs have previously been isolated from patients with rheumatoid arthritis who have received Gold sodium thiomalate (38). These TCRs were present in both $CD4^+$ and $CD8^+$ T-cells and some TCRVβ genes were overrepresented in gold-reactive TCRs. It has been suggested that gold reactivity is based on different mechanisms including covalent binding to large self-derived proteins (cell membrane proteins/MHC peptide complexes) when they are presented by APC, with or without processing. In other scenarios, metals can cross-link TCR to MHC independently of the nature of associated peptide. Gold may even bind and stimulate TCRs independently of MHC (38). However, others have found that gold-reactive TCRs require a compatible MHC (39).

Intriguingly in our study, all four tested participants exhibited a positive skin patch hypersensitivity test to gold thiosulphate as previously reported (2). Most cases of gold allergy involve delayed-type hypersensitivity (40), present in up to 15% of the population (41). It has been hypothesized that MHC-class I-independent $CD8^+$ T-cell responses in response to gold-sensitized APCs is likely related to NKT-cell activation (42). However, in other metal allergies, conventional T-cells are implicated, in many cases with specific TCR sequences or V gene usages (43). We did not observe NKT-cells, and our clonally expanded $CD8^+$ T-cells had a conventional phenotype. It is unclear how a positive gold skin patch test (of generally unclear clinical relevance (37, 44)) relates to the finding of gold-reactive clones in our study. Importantly, systemic hypersensitivity was not observed in any of the participants receiving C19-A3 GNP (2).

There were a significant number of clonal expansions of unknown antigen specificity. We speculate that these could be specific to other epitopes in the C19-A3 GNP compound or to unrelated antigens found in the skin. In addition, as responsiveness to antigens by TCR transduced cells may be lost due to the joining of human TCR to constant regions of the murine TCR, it is possible that specificity for PI or GNP was not detected in our assay system. In addition, in the pancreatic islets 14 out of 187 CD4+ T-cell receptor (TCR) clonotypes responded to pre-proinsulin peptides (with four of six donors having pre-proinsulin specific CD4+ T-cells) (45). In the pancreas of people with T1D between 3% and 40% of the CD8+T-cells are reactive to proinsulin and often exhibit large clonal expansions (26). However, in our data it was surprising that some of the largest clonal expansions were non-specific to the tested antigens.

We next wanted to determine phenotype of blister fluid cells and found that they had features along a spectrum of effector and memory phenotypes, with little evidence of naïve or exhausted phenotypes (8, 46, 47) (Supplementary Figures 1C, D). Only the $CD8^+$ T_{PM} set showed evidence of naivety with expression of CCR7, CD62L and IL7R (Supplementary Figure 1C). Whilst only the $CD8^+$ $T_{RM/EM}$ population was actively proliferating ($Ki67^+$), no subsets had substantial expression of CD57. Although many subsets expressed CD27, none had a $CD27^+CD95^+CCR7^+$ phenotype characteristic of T_{SCM} (8). Whilst we were not able to assess a functional response in our $CD8^+$ T-cells, they were transcriptionally active for a number of cytotoxic transcripts, including GzmB, perforin and GNLY, suggesting that they were participating in an ongoing immune reaction and are more homologous to those found in the islets than normal skin resident $CD8^+$ T-cells. Indeed, previous research into skin resident $CD8^+$ T-cells has indicated that they are phenotypically distinct from those in the peripheral blood and lack immediate cytotoxic functions (48). In contrast, a cytotoxic phenotype was observed in our PI-specific $CD8^+$ clones, as evidenced by DEG analysis, which revealed overexpression in GNLY and KIR receptors in comparison to gold-specific and clones of unknown specificity. KIRs interact with HLA molecules and KIRs with DL tails express immunoreceptor tyrosine-based inhibitory motifs. Significant differences in KIR gene DEG expression is an important finding, as polymorphism in those genes has been associated with T1D, with some genes being identified as protective and others as susceptibility factors for T1D (49–56). For example, children with T1D have fewer inhibitory KIRs with their corresponding ligands compared with healthy control children (55). As the expression of inhibitory KIRs is generally negatively associated with T1D, it is intriguing to see these overrepresented in the PI-specific $CD8^+$ T-cells. However, it is known that the specificity of KIR expressed on $CD8^+$ T-cells is random and often distinct compared with those expressed on NK cells within the same individual (49) and that KIR2DL1 expressing $CD8^+$ T-cells have enhanced cytotoxic capabilities (50). Indeed, PI-specific clones consistently

overexpressed KIR2DL1 in comparison to gold-specific and clones of unknown specificity. Whilst the number of clones included in this analysis was limited, it demonstrates an important proof of principle of how *in vivo* activation and enrichment can be combined with scRNAseq to phenotype diabetes autoantigen-specific T-cells. Although some blister clones showed regulatory properties, this was not the predominant phenotype.

It is open to speculation if the blister clones reactive to injected antigens derived from naive T-cells following antigen stimulation or arrived in the skin from a pre-existing memory pool following antigen stimulation, and if so whether this memory pool was drawn from pancreatic islets or LNs. The appearance of the skin induration approximately 2 weeks after the first injection, but subsequently a much faster skin reaction after the 2nd and 3rd (1-3 days), potentially indicates that the cells have at least proliferated *in situ*. The presence of gold-reactive clones also supports this. Interestingly, we observed different phenotypes with the same clonotype indicating the transformation from effector to long-lasting tissue resident phenotype as a consequence of chronic antigen exposure (57, 58). Our data demonstrate that the phenotypes of the infiltrating T-cell population and more specifically, PI-reactive T-cells, found in blister fluid following C19-A3 GNP injection, more closely resembled the phenotypes of antigen-specific T-cells isolated from human pancreatic islets (Supplementary Figure 1E, F) (59) than those isolated from blood of people with T1D. Studies on diabetes antigen-specific CD8+ T-cells from the peripheral blood of people with T1D displayed remarkably heterogenous phenotypes both within and between individuals, including naïve, memory and exhausted phenotypes (60) as well as effector and stem cell memory T-cells (T_{SCM}) phenotypes that were enriched in people with T1D compared to controls (8). On the other hand, even in donors without diabetes, T-cells infiltrating the pancreas are dominated by CD8$^+$ T-cells that display memory and effector memory phenotypes with markers of tissue residency (61). Others have reported that, in healthy donors, pancreatic T-cells are largely T_{RM}, expressing CD127 (a marker of long-lived memory and antigen-independent replication), with no features of exhaustion and no CD57 expression, also expressing high levels of PD-1, GzmB, CD101, CD49a and CD103 compared to those in the peripheral lymph nodes (PLN) (62). Pancreatic T-cells had highly expanded clonotypes, whereas those in the PLN had a greater diversity (19, 62). A comparison between islet-infiltrating cells in healthy donors and those with T1D found that CD8$^+$$T_{RM}$ cells were more abundant in people with diabetes. T_{RM} dominated the infiltrate (43% of CD8$^+$ T-cells were CD69$^+$CD103$^+$) and there were relatively few effector CD8$^+$ without features of tissue residency and memory (63).

A limitation of the study is the small number of participants that emphasizes individual differences in immune response. In addition, post-injection timing of the samples had a wide range from 3-7 months for biopsies and 10-28 months for suction blisters. Therefore, comparisons are made between different stages of the immunological response to C19-A3 GNP, although late sampling time-points in all individuals make it more likely that processes were in the stage of tissue residency in all participants.

Antigen-specific cells remained enriched and *in situ* for 10-28 months post treatment with C19-A3 GNP. It is likely that injection and chronic skin retention of this compound induced the conversion and proliferation of naive antigen-specific T-cells to a cytotoxic tissue-resident phenotype rather than recirculation of pre-existing memory cells to the skin. Long-term retention in the skin opens the possibility of a novel opportunity for sustained immune modulation using GNPs to deliver antigens. Further work is required to optimize compound characteristics to favor tolerogenic properties, essential for autoimmune diseases. For example, we have previously shown that minimally invasive intradermal delivery of diabetes autoantigens and pre-treatment of skin with steroids promotes tolerance for treatment of T1D (21, 29, 64). However, the system maybe already suitable in its current form for delivering traditional immune-stimulating vaccines. This is because this platform includes both intradermal delivery and extended duration of antigen presentation known to promote generation of $T_{RM,}$ important for vaccine effectiveness (58).

In summary, by using novel scRNAseq technology we have shown that intradermal administration of peptide-gold nanoparticle resulted in recruitment and clonal expansion of antigen-specific T-cells. This opens a wide range of possibilities for application of this methodology in clinical practice.

Data availability statement

Bulk RNAseq is deposited in ArrayExpress accession E-MTAB-13386, scRNASeq is deposited in ArrayExpress accession E-MTAB-13388.

Ethics statement

The studies involving humans were approved by Sweden : Regionala Etikprovningsnamenden Linkoping (EPN),reference: 2015/439-31. UK: London - City & East Research Ethics Committee, reference: 16/LO/0020. The studies were conducted in accordance with the local legislation and institutional requirements. The participants provided their written informed consent to participate in this study.

Author contributions

SH: Conceptualization, Formal Analysis, Investigation, Methodology, Writing – original draft, Writing – review and editing. TCT: Conceptualization, Investigation, Methodology, Writing – review and editing. ER: Investigation, Methodology, Writing – review and editing. NV: Investigation, Methodology, Writing – review and editing. NW: Methodology, Supervision, Writing – review and editing. LL: Conceptualization, Methodology, Writing – review and editing. RA: Formal Analysis, Methodology, Writing – review and editing. QS: Investigation, Writing – review and editing. PL: Formal Analysis, Investigation, Methodology, Writing – review and editing. RW: Formal Analysis, Investigation, Methodology, Writing – review and editing. MM: Conceptualization, Methodology, Writing – review and editing.

MN: Investigation, Methodology, Writing – review and editing. FW: Conceptualization, Supervision, Writing – review and editing. JY: Investigation, Methodology, Writing – review and editing. TIMT: Methodology, Supervision, Writing – review and editing. JL: Supervision, Writing – review and editing. CD: Conceptualization, Funding acquisition, Supervision, Writing – original draft, Writing – review and editing. DT: Conceptualization, Formal Analysis, Investigation, Methodology, Writing – original draft, Writing – review and editing.

Funding

The author(s) declare financial support was received for the research, authorship, and/or publication of this article. EE-ASI was a European research network Collaborative Project supported by the European Commission under the Health Cooperation Work Programme of the 7th Framework Programme, under the Grant Agreement 305305.

Acknowledgments

SH is funded by the Diabetes Research and Wellness Foundation Professor David Matthews Non-Clinical Research Fellowship. PL is funded by the Diabetes UK RD Lawrence Fellowship. ER is funded by a grant from the Leona M. and Harry B. Helmsley Charitable Trust. QS was funded by a Society for Endocrinology summer studentship.

Conflict of interest

CD has lectured for or been involved as an advisor to the following companies: Novonordisk, Sanofi-genzyme, Janssen, Servier, Lilly, Astrazeneca, Provention Bio, UCB, MSD, Vielo Bio, Avotres, Worg, Novartis. CD holds a patent jointly with Midatech plc and Provention Bio/Sanofi. DT is a Trustee for NovoNordisk UK Research Foundation.

The remaining authors declare that the research was conducted in the absence of any commercial or financial relationships that could be construed as a potential conflict of interest.

Publisher's note

Supplementary material

The Supplementary Material for this article can be found online at: https://www.frontiersin.org/articles/10.3389/fimmu.2023.1276255/full#supplementary-material

References

1. Dul M, Nikolic T, Stefanidou M, McAteer MA, Williams P, Mous J, et al. Conjugation of a peptide autoantigen to gold nanoparticles for intradermally administered antigen specific immunotherapy. *Int J Pharm* (2019) 562:303–12. doi: 10.1016/j.ijpharm.2019.03.041

2. Tatovic D, McAteer MA, Barry J, Barrientos A, Rodriguez Terradillos K, Perera I, et al. Safety of the use of gold nanoparticles conjugated with proinsulin peptide and administered by hollow microneedles as an immunotherapy in type 1 diabetes. *Immunother Adv* (2022) 2(1):ltac002. doi: 10.1093/immadv/ltac002

3. Thrower SL, James L, Hall W, Green KM, Arif S, Allen JS, et al. Proinsulin peptide immunotherapy in type 1 diabetes: report of a first-in-man Phase I safety study. *Clin Exp Immunol* (2009) 155(2):156–65. doi: 10.1111/j.1365-2249.2008.03814.x

4. Alhadj Ali M, Liu YF, Arif S, Tatovic D, Shariff H, Gibson VB, et al. Metabolic and immune effects of immunotherapy with proinsulin peptide in human new-onset type 1 diabetes. *Sci Transl Med* (2017) 9(402). doi: 10.1126/scitranslmed.aaf7779

5. Merad M, Ginhoux F, Collin M. Origin, homeostasis and function of Langerhans cells and other langerin-expressing dendritic cells. *Nat Rev Immunol* (2008) 8(12):935–47. doi: 10.1038/nri2455

6. Steinman RM, Hawiger D, Nussenzweig MC. Tolerogenic dendritic cells. *Annu Rev Immunol* (2003) 21:685–711. doi: 10.1146/annurev.immunol.21.120601.141040

7. Eugster A, Lindner A, Catani M, Heninger AK, Dahl A, Klemroth S, et al. High diversity in the TCR repertoire of GAD65 autoantigen-specific human CD4+ T cells. *J Immunol* (2015) 194(6):2531–8. doi: 10.4049/jimmunol.1403031

8. Skowera A, Ladell K, McLaren JE, Dolton G, Matthews KK, Gostick E, et al. beta-cell-specific CD8 T cell phenotype in type 1 diabetes reflects chronic autoantigen exposure. *Diabetes* (2015) 64(3):916–25. doi: 10.2337/db14-0332

9. Hanna SJ, Powell WE, Long AE, Robinson EJS, Davies J, Megson C, et al. Slow progressors to type 1 diabetes lose islet autoantibodies over time, have few islet antigen-specific CD8(+) T cells and exhibit a distinct CD95(hi) B cell phenotype. *Diabetologia* (2020) 63(6):1174–85. doi: 10.1007/s00125-020-05114-7

10. Ahmed S, Cerosaletti K, James E, Long SA, Mannering S, Speake C, et al. Standardizing T-cell biomarkers in type 1 diabetes: challenges and recent advances. *Diabetes* (2019) 68(7):1366–79. doi: 10.2337/db19-0119

11. James EA, Mallone R, Kent SC, DiLorenzo TP. T-cell epitopes and neo-epitopes in type 1 diabetes: A comprehensive update and reappraisal. *Diabetes* (2020) 69 (7):1311–35. doi: 10.2337/dbi19-0022

12. Arif S, Pujol-Autonell I, Kamra Y, Williams E, Yusuf N, Domingo-Vila C, et al. Mapping T cell responses to native and neo-islet antigen epitopes in at risk and type 1 diabetes subjects. *Front Immunol* (2021) 12:675746. doi: 10.3389/fimmu.2021.675746

13. Cerosaletti K, Barahmand-Pour-Whitman F, Yang J, DeBerg HA, Dufort MJ, Murray SA, et al. Single-cell RNA sequencing reveals expanded clones of islet antigen-reactive CD4(+) T cells in peripheral blood of subjects with type 1 diabetes. *J Immunol* (2017) 199(1):323–35. doi: 10.4049/jimmunol.1700172

14. Penkava F, Velasco-Herrera MDC, Young MD, Yager N, Nwosu LN, Pratt AG, et al. Single-cell sequencing reveals clonal expansions of pro-inflammatory synovial CD8 T cells expressing tissue-homing receptors in psoriatic arthritis. *Nat Commun* (2020) 11(1):4767. doi: 10.1038/s41467-020-18513-6

15. Michels AW, Landry LG, McDaniel KA, Yu L, Campbell-Thompson M, Kwok WW, et al. Islet-derived CD4 T cells targeting proinsulin in human autoimmune diabetes. *Diabetes* (2017) 66(3):722–34. doi: 10.2337/db16-1025

16. Hanna SJ, Tatovic D, Thayer TC, Dayan CM. Insights from single cell RNA sequencing into the immunology of type 1 diabetes- cell phenotypes and antigen specificity. *Front Immunol* (2021) 12:751701. doi: 10.3389/fimmu.2021.751701

17. Kent SC, Chen Y, Bregoli L, Clemmings SM, Kenyon NS, Ricordi C, et al. Expanded T cells from pancreatic lymph nodes of type 1 diabetic subjects recognize an insulin epitope. *Nature* (2005) 435(7039):224–8. doi: 10.1038/nature03625

18. Pathiraja V, Kuehlich JP, Campbell PD, Krishnamurthy B, Loudovaris T, Coates PT, et al. Proinsulin-specific, HLA-DQ8, and HLA-DQ8-transdimer-restricted CD4+ T cells infiltrate islets in type 1 diabetes. *Diabetes* (2015) 64(1):172–82. doi: 10.2337/db14-0858

19. Seay HR, Yusko E, Rothweiler SJ, Zhang L, Posgai AL, Campbell-Thompson M, et al. Tissue distribution and clonal diversity of the T and B cell repertoire in type 1 diabetes. *JCI Insight* (2016) 1(20):e88242. doi: 10.1172/jci.insight.88242

20. Singh RK, Malosse C, Davies J, Malissen B, Kochba E, Levin Y, et al. Using gold nanoparticles for enhanced intradermal delivery of poorly soluble auto-antigenic peptides. *Nanomedicine* (2021) 32:102321. doi: 10.1016/j.nano.2020.102321

21. Ali MA, Thrower SL, Hanna SJ, Coulman SA, Birchall JC, Wong FS, et al. Topical steroid therapy induces pro-tolerogenic changes in Langerhans cells in human skin. *Immunology* (2015) 146(3):411–22. doi: 10.1111/imm.12518

22. Stuart T, Butler A, Hoffman P, Hafemeister C, Papalexi E, Mauck WM 3rd, et al. Comprehensive integration of single-cell data. *Cell* (2019) 177(7):1888–902 e21. doi: 10.1016/j.cell.2019.05.031

23. McGinnis CS, Murrow LM, Gartner ZJ. DoubletFinder: doublet detection in single-cell RNA sequencing data using artificial nearest neighbors. *Cell Syst* (2019) 8 (4):329–37 e4. doi: 10.1016/j.cels.2019.03.003

24. Shugay M, Bagaev DV, Zvyagin IV, Vroomans RM, Crawford JC, Dolton G, et al. VDJdb: a curated database of T-cell receptor sequences with known antigen specificity. *Nucleic Acids Res* (2018) 46(D1):D419–D27. doi: 10.1093/nar/gkx760

25. Tickotsky N, Sagiv T, Prilusky J, Shifrut E, Friedman N. McPAS-TCR: a manually curated catalogue of pathology-associated T cell receptor sequences. *Bioinformatics* (2017) 33(18):2924–9. doi: 10.1093/bioinformatics/btx286

26. Anderson AM, Landry LG, Alkanani AA, Pyle L, Powers AC, Atkinson MA, et al. Human islet T cells are highly reactive to preproinsulin in type 1 diabetes. *Proc Natl Acad Sci U S A* (2021) 118(41). doi: 10.1073/pnas.2107208118

27. Mann SE, Zhou Z, Landry LG, Anderson AM, Alkanani AK, Fischer J, et al. Multiplex T cell stimulation assay utilizing a T cell activation reporter-based detection system. *Front Immunol* (2020) 11:633. doi: 10.3389/fimmu.2020.00633

28. Zhou Y, Zhou B, Pache L, Chang M, Khodabakhshi AH, Tanaseichuk O, et al. Metascape provides a biologist-oriented resource for the analysis of systems-level datasets. *Nat Commun* (2019) 10(1):1523. doi: 10.1038/s41467-019-09234-6

29. Arikat F, Hanna SJ, Singh RK, Vilela L, Wong FS, Dayan CM, et al. Targeting proinsulin to local immune cells using an intradermal microneedle delivery system; a potential antigen-specific immunotherapy for type 1 diabetes. *J Control Release* (2020) 322:593–601. doi: 10.1016/j.jconrel.2020.02.031

30. Redmond D, Poran A, Elemento O. Single-cell TCRseq: paired recovery of entire T-cell alpha and beta chain transcripts in T-cell receptors from single-cell RNAseq. *Genome Med* (2016) 8(1):80. doi: 10.1186/s13073-016-0335-7

31. Landry LG, Mann SE, Anderson AM, Nakayama M. Multiplex T-cell stimulation assay utilizing a T-cell activation reporter-based detection system. *Bio Protoc* (2021) 11 (2):e3883. doi: 10.21769/BioProtoc.3883

32. Arif S, Tree TI, Astill TP, Tremble JM, Bishop AJ, Dayan CM, et al. Autoreactive T cell responses show proinflammatory polarization in diabetes but a regulatory phenotype in health. *J Clin Invest* (2004) 113(3):451–63. doi: 10.1172/JCI19585

33. Sidney J, Vela JL, Friedrich D, Kolla R, von Herrath M, Wesley JD, et al. Low HLA binding of diabetes-associated CD8+ T-cell epitopes is increased by post translational modifications. *BMC Immunol* (2018) 19(1):12. doi: 10.1186/s12865-018-0250-3

34. Chang L, Kjer-Nielsen L, Flynn S, Brooks AG, Mannering SI, Honeyman MC, et al. Novel strategy for identification of candidate cytotoxic T-cell epitopes from human preproinsulin. *Tissue Antigens* (2003) 62(5):408–17. doi: 10.1034/j.1399-0039.2003.00122.x

35. Unger WW, Velthuis J, Abreu JR, Laban S, Quinten E, Kester MG, et al. Discovery of low-affinity preproinsulin epitopes and detection of autoreactive CD8 T-cells using combinatorial MHC multimers. *J Autoimmun* (2011) 37(3):151–9. doi: 10.1016/j.jaut.2011.05.012

36. Kronenberg D, Knight RR, Estorninho M, Ellis RJ, Kester MG, de Ru A, et al. Circulating preproinsulin signal peptide-specific CD8 T cells restricted by the susceptibility molecule HLA-A24 are expanded at onset of type 1 diabetes and kill beta-cells. *Diabetes* (2012) 61(7):1752–9. doi: 10.2337/db11-1520

37. Chen JK, Lampel HP. Gold contact allergy: clues and controversies. *Dermatitis* (2015) 26(2):69–77. doi: 10.1097/DER.0000000000000101

38. Hashizume H, Seo N, Ito T, Takigawa M, Yagi H. Promiscuous interaction between gold-specific T cells and APCs in gold allergy. *J Immunol* (2008) 181 (11):8096–102. doi: 10.4049/jimmunol.181.11.8096

39. Romagnoli P, Spinas GA, Sinigaglia F. Gold-specific T cells in rheumatoid arthritis patients treated with gold. *J Clin Invest* (1992) 89(1):254–8. doi: 10.1172/JCI115569

40. Bjorklund G, Dadar M, Aaseth J. Delayed-type hypersensitivity to metals in connective tissue diseases and fibromyalgia. *Environ Res* (2018) 161:573–9. doi: 10.1016/j.envres.2017.12.004

41. Suzuki K, Yagami A, Ito A, Kato A, Miyazawa H, Kanto H, et al. Positive reactions to gold sodium thiosulfate in patch test panels (TRUE Test) in Japan: A multicentre study. *Contact Dermatitis* (2019) 80(2):114–7. doi: 10.1111/cod.13105

42. de Lima Moreira M, Souter MNT, Chen Z, Loh L, McCluskey J, Pellicci DG, et al. Hypersensitivities following allergen antigen recognition by unconventional T cells. *Allergy* (2020) 75(10):2477–90. doi: 10.1111/all.14279

43. Takeda Y, Suto Y, Ito K, Hashimoto W, Nishiya T, Ueda K, et al. TRAV7-2*02 expressing CD8(+) T cells are responsible for palladium allergy. *Int J Mol Sci* (2017) 18 (6). doi: 10.3390/ijms18061162

44. Bruze M, Edman B, Bjorkner B, Moller H. Clinical relevance of contact allergy to gold sodium thiosulfate. *J Am Acad Dermatol* (1994) 31(4):579–83. doi: 10.1016/S0190-9622(94)70219-5

45. Landry LG, Anderson AM, Russ HA, Yu L, Kent SC, Atkinson MA, et al. Proinsulin-reactive CD4 T cells in the islets of type 1 diabetes organ donors. *Front Endocrinol (Lausanne)* (2021) 12:622647. doi: 10.3389/fendo.2021.622647

46. Blank CU, Haining WN, Held W, Hogan PG, Kallies A, Lugli E, et al. Defining 'T cell exhaustion'. *Nat Rev Immunol* (2019) 19(11):665–74. doi: 10.1038/s41577-019-0221-9

47. Ahmed R, Miners KL, Lahoz-Beneytez J, Jones RE, Roger L, Baboonian C, et al. CD57(+) memory T cells proliferate *in vivo*. *Cell Rep* (2020) 33(11):108501. doi: 10.1016/j.celrep.2020.108501

48. Seidel JA, Vukmanovic-Stejic M, Muller-Durovic B, Patel N, Fuentes-Duculan J, Henson SM, et al. Skin resident memory CD8(+) T cells are phenotypically and functionally distinct from circulating populations and lack immediate cytotoxic function. *Clin Exp Immunol* (2018) 194(1):79–92. doi: 10.1111/cei.13189

49. Bjorkstrom NK, Beziat V, Cichocki F, Liu LL, Levine J, Larsson S, et al. CD8 T cells express randomly selected KIRs with distinct specificities compared with NK cells. *Blood* (2012) 120(17):3455–65. doi: 10.1182/blood-2012-03-416867

50. Gimeno L, Serrano-Lopez EM, Campillo JA, Canovas-Zapata MA, Acuna OS, Garcia-Cozar F, et al. KIR+ CD8+ T lymphocytes in cancer immunosurveillance and patient survival: gene expression profiling. *Cancers (Basel)* (2020) 12(10). doi: 10.3390/cancers12102991

51. Soltani S, Mostafaei S, Aslani S, Farhadi E, Mahmoudi M. Association of KIR gene polymorphisms with Type 1 Diabetes: a meta-analysis. *J Diabetes Metab Disord* (2020) 19(2):1777–86. doi: 10.1007/s40200-020-00569-2

52. Osman AE, Eltayeb EN, Mubasher M, Al Harthi H, Alharbi S, Hamza MA, et al. Investigation of activating and inhibitory killer cell immunoglobulin-like receptors and their putative ligands in type 1 diabetes (T1D). *Hum Immunol* (2016) 77(1):110–4. doi: 10.1016/j.humimm.2015.10.019

53. Jobim M, Chagastelles P, Salim PH, Portela P, Wilson TJ, Curti AG, et al. Association of killer cell immunoglobulin-like receptors and human leukocyte antigen-C genotypes in South Brazilian with type 1 diabetes. *Hum Immunol* (2010) 71(8):799–803. doi: 10.1016/j.humimm.2010.05.014

54. Zhi D, Sun C, Sedimbi SK, Luo F, Shen S, Sanjeevi CB. Killer cell immunoglobulin-like receptor along with HLA-C ligand genes are associated with type 1 diabetes in Chinese Han population. *Diabetes Metab Res Rev* (2011) 27(8):872–7. doi: 10.1002/dmrr.1264

55. Mehers KL, Long AE, van der Slik AR, Aitken RJ, Nathwani V, Wong FS, et al. An increased frequency of NK cell receptor and HLA-C group 1 combinations in early-onset type 1 diabetes. *Diabetologia* (2011) 54(12):3062–70. doi: 10.1007/s00125-011-2299-x

56. Lin L, Ma C, Wei B, Aziz N, Rajalingam R, Yusung S, et al. Human NK cells licensed by killer Ig receptor genes have an altered cytokine program that modifies CD4 + T cell function. *J Immunol* (2014) 193(2):940–9. doi: 10.4049/jimmunol.1400093

57. Tokura Y, Phadungsaksawasdi P, Kurihara K, Fujiyama T, Honda T. Pathophysiology of skin resident memory T cells. *Front Immunol* (2020) 11:618897. doi: 10.3389/fimmu.2020.618897

58. Rotrosen E, Kupper TS. Assessing the generation of tissue resident memory T cells by vaccines. *Nat Rev Immunol* (2023) 1-11. doi: 10.1038/s41577-023-00853-1

59. Nakayama M, Michels AW. Determining antigen specificity of human islet infiltrating T cells in type 1 diabetes. *Front Immunol* (2019) 10:365. doi: 10.3389/fimmu.2019.00365

60. Laban S, Suwandi JS, van Unen V, Pool J, Wesselius J, Hollt T, et al. Heterogeneity of circulating CD8 T-cells specific to islet, neo-antigen and virus in patients with type 1 diabetes mellitus. *PloS One* (2018) 13(8):e0200818. doi: 10.1371/journal.pone.0200818

61. Radenkovic M, Uvebrant K, Skog O, Sarmiento L, Avartsson J, Storm P, et al. Characterization of resident lymphocytes in human pancreatic islets. *Clin Exp Immunol* (2017) 187(3):418–27. doi: 10.1111/cei.12892

62. Weisberg SP, Carpenter DJ, Chait M, Dogra P, Gartrell-Corrado RD, Chen AX, et al. Tissue-resident memory T cells mediate immune homeostasis in the human pancreas through the PD-1/PD-L1 pathway. *Cell Rep* (2019) 29(12):3916–32 e5. doi: 10.1016/j.celrep.2019.11.056

63. Kuric E, Seiron P, Krogvold L, Edwin B, Buanes T, Hanssen KF, et al. Demonstration of tissue resident memory CD8 T cells in insulitic lesions in adult patients with recent-onset type 1 diabetes. *Am J Pathol* (2017) 187(3):581–8. doi: 10.1016/j.ajpath.2016.11.002

64. Zhao X, Birchall JC, Coulman SA, Tatovic D, Singh RK, Wen L, et al. Microneedle delivery of autoantigen for immunotherapy in type 1 diabetes. *J Control Release* (2016) 223:178–87. doi: 10.1016/j.jconrel.2015.12.040